

Published in final edited form as:

Islets. 2009 September ; 1(2): 129–136. doi:10.4161/isl.1.2.9480.

## Islet architecture:

### A comparative study

Abraham Kim<sup>1</sup>, Kevin Miller<sup>1</sup>, Junghyo Jo<sup>2</sup>, German Kilimnik<sup>1</sup>, Pawel Wojcik<sup>1</sup>, and Manami Hara<sup>1,\*</sup>

<sup>1</sup>Department of Medicine; The University of Chicago; Chicago, IL USA

<sup>2</sup>Laboratory of Biological Modeling; National Institute of Diabetes and Digestive and Kidney Diseases; National Institutes of Health; Bethesda, MD USA

### Abstract

Emerging reports on the organization of the different hormone-secreting cell types ( $\alpha$ , glucagon;  $\beta$ , insulin; and  $\delta$ , somatostatin) in human islets have emphasized the distinct differences between human and mouse islets, raising questions about the relevance of studies of mouse islets to human islet physiology. Here, we examine the differences and similarities between the architecture of human and mouse islets. We studied islets from various mouse models including *ob/ob* and *db/db* and pregnant mice. We also examined the islets of monkeys, pigs, rabbits and birds for further comparisons. Despite differences in overall body and pancreas size as well as total  $\beta$ -cell mass among these species, the distribution of their islet sizes closely overlaps, except in the bird pancreas in which the  $\delta$ -cell population predominates (both in singlets and clusters) along with a small number of islets. Markedly large islets ( $>10,000 \mu\text{m}^2$ ) were observed in human and monkey islets as well as in islets from *ob/ob* and pregnant mice. The fraction of  $\alpha$ -,  $\beta$ - and  $\delta$ -cells within an islet varied between islets in all the species examined. Furthermore, there was variability in the distribution of  $\alpha$ - and  $\delta$ -cells within the same species. In summary, human and mouse islets share common architectural features that may reflect demand for insulin. Comparative studies of islet architecture may lead to a better understanding of islet development and function.

### Keywords

pancreatic islets;  $\beta$ -cells;  $\alpha$ -cells;  $\delta$ -cells; pregnancy; insulin resistance; diabetes

### Introduction

The pancreatic islet is composed of multiple cell types, including insulin-secreting  $\beta$ -cells, glucagon-secreting  $\alpha$ -cells and somatostatin-secreting  $\delta$ -cells, which work together in this micro-organ to maintain normoglycemia. Recently, notable cytoarchitectural differences between mouse and human islets have been reported.<sup>1,2</sup> In islets from mice and other rodents, the  $\beta$ -cells are located predominately in the central core with  $\alpha$ - and  $\delta$ -cells localized in the periphery forming a mantle.<sup>3-7</sup> In human and monkey islets, the  $\alpha$ -cells are not localized in the periphery but are rather dispersed throughout the islet.<sup>1,2,6-8</sup> The organization of the  $\beta$ - and  $\alpha$ -cells in dogs and pigs is an intermediate between that in rodents and monkeys with occasional appearances of  $\alpha$ -cells in the central core.<sup>6,9-11</sup>

The “disorganized” cellular composition of islets in primates (both humans and monkeys) has been suggested to affect  $\beta$ -cell function by allowing these cells to respond to low concentrations of glucose (1 mM) to which normal mouse islets are blind.<sup>2</sup> Here, we examine the architecture of pancreatic islets in a diverse group of animals (human, monkey, pig, rabbit, bird, mouse) and the notion of a prototypic islet.

It is well known that there is a close correlation between body and pancreas weight. Total  $\beta$ -cell mass also increases proportionately to compensate the demand for insulin in the body.<sup>12, 13</sup> What escapes this proportionate expansion is the size distribution of islets. Large animals such as humans share similar islet sizes with mice,<sup>14,15</sup> suggesting that this micro-organ has a certain size limit to be functional. The inability of large animal pancreata to generate gigantic islets can be compensated by an increase in the number of islets. We hypothesized that such compensation could also have occurred by an enhancement in islet function, which might reflect changes in islet architecture and composition reported in human and monkey islets.<sup>1,2</sup> The distinct arrangement of a central core of  $\beta$ -cells and peripheral  $\alpha$ -cells has been suggested to be functionally coupled to the pattern of blood flow in the islet.<sup>16-18</sup> If there is an association between islet architecture and a microcirculatory pattern, the organization of endocrine cells within the islet should be similar in all the islets of that species although there could be differences between species.

In the present study, we aim to validate the notion that there are fundamental differences in islet architecture and composition between species. We extended the comparison not only to between humans and mice, but also among various species. In addition, mice in states of increased demand for insulin such as obesity, pregnancy and diabetes were examined. Here we report the significant plasticity of islet cytoarchitecture throughout the species examined, which previously may not have been fully appreciated. Within a certain limit of islet size, the overall changes observed in islet structure may reflect the islet adaptation to the increased body demands rather than species differences.

## Results

### Comparison of islet architecture and composition among different species

We carried out a comparative study on islet architecture and composition among various species: human ( $39 \pm 4.2$  yr), monkey (1-yr), pig (6-mo), rabbit (6-mo), mouse (6-mo) and bird (40-d). We also studied islets from various mouse models including *ob/ob* (15-wk), *db/db* (15-wk) and pregnant (3-mo) mice. While overall body size as well as pancreas size and total  $\beta$ -cell mass significantly differ among these species, their islet size distributions fall into a similar range (Fig. 1A). A large number of small clusters of endocrine cells ( $<2,000 \mu\text{m}^2$ ) was observed across the species examined, followed by a similar regression in frequency of larger islets. Markedly large islets ( $>10,000 \mu\text{m}^2$ ) were present in human and monkey pancreata as well as in those of rabbits, *ob/ob* and pregnant mice. Figure 1B shows an overview of islet distribution in each species. They all exhibit a similar pattern of distribution, where various sizes of islets are scattered including small clusters of endocrine cells (Fig. 1B, a-e). In the bird pancreas, however, a relatively small number of islets containing  $\beta$ -cells are found and the  $\delta$ -cell population predominates (Fig. 1B, f). The fraction of  $\alpha$ -,  $\beta$ - and  $\delta$ -cells within an islet varied between islets in all of the species examined; where some islets were mainly composed of  $\beta$ -cells, while some had a mixed composition with  $\alpha$ - and  $\delta$ -cells, exhibiting the diversity of islet architecture and composition (Fig. 2). The distinct difference observed between human and monkey islets and those of wild-type mice, in particular, is that the frequency of islets with a mixed endocrine population is higher in primates. Note that pig islets differ from the rest of the species. No large islets comparable to those found in rabbits, obese or pregnant mice were observed (Fig. 1A), and the overall islet architecture appears less compacted (Fig. 2). For a detailed comparison of islet size and cell composition among species, we plotted for islet sizes

(Fig. 3). In order to display a clear comparison of islet size, we used an “effective diameter” determined from a circle that gives an area corresponding to a measured islet area. It is of interest that every islet size distribution fits reasonably with the lognormal distribution function, suggesting a common islet growth mechanism among species. The statistics of effective islet size,  $\beta$ -cell ratio, and two parameters of the lognormal function are summarized in Table 1 for all the species. Compared to mice, islets of other species have compact size ranges, which is also reflected in the scale parameter,  $\sigma$ , of the lognormal function; the values for mice are larger than the ones for other species. Human islets have a relatively small  $\beta$ -cell fraction compared to other species. Furthermore, as islet size increases, the  $\beta$ -cell fraction decreases in human islets (Fig. 3).

### Changes in islet architecture and composition under pathophysiological conditions

The comparative study on islet architecture and composition among various species described above suggested a certain limit in size for this micro-organ to grow and be functional. We hypothesized that a similar change seen in primate islets to compensate for body demand with a limited islet size might also occur in mice in response to an increased demand for insulin under conditions such as obesity, pregnancy and diabetes. An overview of islet distribution in *ob/ob* mice shows a number of large islets (average body weight:  $54.5 \pm 2.3$  g and blood glucose level:  $169 \pm 24$  mg/dL at 15-wk; Fig. 4A, a), whose size is equivalent to that of a subpopulation of primate islets (Fig. 1A). Such large islets are also observed in pregnant mice (Figs. 4A, b and 1A). In some *ob/ob* and pregnant mouse islets,  $\alpha$ - and  $\delta$ -cells are intermingled with  $\beta$ -cells (Fig. 4), as opposed to the typical islet composition seen in mice under normal conditions, where they are more localized in the periphery (Fig. 2). This change in endocrine cell composition is prominent in obese and diabetic *db/db* mice (average body weight:  $40.7 \pm 1.1$  g and blood glucose level:  $388 \pm 22$  mg/dL at 15-wk), in which  $\alpha$ - and  $\delta$ -cells are widely mixed with  $\beta$ -cells within an islet (Fig. 4A, c). In particular, islet size and  $\beta$ -cell ratio of *db/db* mice are similar with the values of human islets (Table 1 and Fig. 3). Note that such a structural change is not accompanied with increased islet size (Fig. 1A). A comparative 3D plot between human and mice under such pathophysiological conditions demonstrates the overall similarities in islet size distribution and islet composition (Fig. 4B, lower right).

## Discussion

### Islet morphology and function

We carried out a comparative study of islet composition and architecture. The range of islet sizes closely overlaps among humans, monkeys, pigs, rabbits and mice. However, islet composition and architecture varies among species. They also vary within the same species under normal conditions. The effect of the differences in cellular composition of islets on function is unknown, especially the relatively high number of  $\delta$  cells in song birds.

The distinct segregation of non- $\beta$ -cells in the periphery of the rodent islets has been an interesting issue because of its implications concerning islet function. The islet is a highly-vascularized micro-organ for its endocrine function. Thus, a reasonable hypothesis was that this specific organization of endocrine cells should determine a microcirculatory pattern for the most efficient signaling within an islet. Collectively, three models have been proposed; (1) Mantle to core: The mantle formation enables non- $\beta$ -cells to sense changes in external glucose concentrations before the signals go to the core of  $\beta$ -cells to secrete sufficient amounts of insulin;<sup>19-23</sup> (2) Core to mantle:  $\beta$ -cells sense the changes first and secrete insulin, then the mantle cells modify the response by counter-acting;<sup>17-18,24</sup> and (3) Artery to vein: following the principal of blood circulation, blood flow enters into an islet from the artery and drains to the vein regardless of the cellular composition.<sup>25-26</sup> While these models are mutually exclusive, Nyman et al. have shown in their elegant study of in vivo microcirculatory imaging

of islet blood flow that all three patterns of blood circulation are observed in mice.<sup>27</sup> They reported that the core to mantle blood flow (Model 2) appeared to be predominant at least in the dorsal pancreas. Nonetheless, the study implies that morphology does not determine microcirculatory patterns of the islet. Our findings showing marked diversity in islet architecture between islets from a single animal across all the species studied here does not support a relationship, at least a simple relationship, between islet architecture and the pattern of blood flow within the islet.

### Islet plasticity under pathophysiological conditions such as obesity, pregnancy and diabetes

We have further shown that physiological and pathological states can affect islet composition and architecture. Increased  $\beta$ -cell mass has been observed in models where there is an increased metabolic demand such as obesity<sup>28,29</sup> and pregnancy.<sup>30,31</sup> Our study of mouse models of obesity and pregnancy reports that total  $\beta$ -cell mass expansion is accompanied with cytoarchitectural changes of the islet. Bock et al. described that the significant increase in  $\beta$ -cell mass in *ob/ob* mice, which bears a mutation in leptin gene, was due to islet hypertrophy, not an increase in the number of islets.<sup>32</sup> It may suggest that individual islets can sense an increased demand for insulin and compensate for it by accelerated  $\beta$ -cell replication and cytoarchitectural reorganization. Similar changes are observed during pregnancy in mice, in which compensatory changes of  $\beta$ -cell mass are tightly regulated by specific gene expressions.<sup>30,31</sup> One of the mouse models of type 2 diabetes, *db/db* mice, which exhibits obesity and diabetes due to a mutation in the leptin receptor, shows a distinct phenotype of islet structure. No large islets comparable to similarly obese *ob/ob* mice were observed, which may reflect relatively mild obesity in *db/db* mice compared to *ob/ob* mice ( $40.7 \pm 1.1$  g and  $54.5 \pm 2.3$  g, respectively at 15-wk). Note that wild-type C57BL/6 mice at 15-wk weigh around 30 g (www.jax.org). However, with overt diabetes (average blood glucose level:  $388 \pm 22$  mg/dL), a majority of islets show extensively intermingled endocrine cell composition with relatively reserved  $\beta$ -cell components within an islet, and an overall size distribution of islets is comparable to that of normal mice and other species. Note that this islet phenotype differs from that of islets with “the collapse of the  $\beta$ -cell core” seen in NOD mice, a mouse model of autoimmune diabetes. In NOD mice with overt diabetes,  $\beta$ -cells within an islet are replaced with infiltrated lymphocytes and only residual  $\alpha$ - and  $\delta$ -cells are observed in an islet-like structure (Hara et al. unpublished data).

### Human versus mouse islets

Histological studies of human islets tend to emphasize the differences between human and mouse islets rather than their similarities. However, studies of human islets are confounded largely by the paucity of human islets and pancreatic tissue for research. Variability of the quality of islets including purity and functionality results in the difficulty of normalizing data generated from specimens from various donors of different ages, ethnic backgrounds and health states. Therefore, simple comparison of human data with that of laboratory animals may be misleading.

In summary, the comparative study on islets in various species has revealed the striking plasticity in islet architecture and composition among species as well as within the same species. We have also shown that such plasticity is seen in response to physiological and pathological changes in the body. Considering the definite size limit of an islet as a micro-organ observed throughout various species, the overall differences of islet architecture and functions (and possibly a certain gene expression), between human and mouse islets in particular, may reflect physiological and evolutionary adjustments to accommodate changing demands for insulin under normal and pathophysiological conditions rather than species differences.

## Materials and Methods

### Animals

Pancreata were obtained from rhesus monkeys (*Macaca mulatta*), Yorkshire farm pigs (*Sus scrofa*), New Zealand white rabbits (*Oryctolagus cuniculus*) and song birds (provided by Dr. Daniel Margoliash). Mouse pancreata were obtained from normal, *ob/ob*, *db/db* and pregnant mice (C57BL/6). All the procedures involving animals were approved by the University of Chicago Institutional Animal Care and Use Committee.

### Human pancreatic tissue slides

Slides with human pancreatic tissue were purchased from the Network for Pancreatic Organ Donors with Diabetes (nPOD). Use of human tissue sections was approved by the University of Chicago Institutional Review Board.

### Immunohistochemistry

Paraffin-embedded sections were cut with a thickness of 6  $\mu\text{m}$ . Sections were stained with a polyclonal guinea pig anti-porcine insulin primary antibody (DAKO, Carpinteria, CA), a mouse monoclonal anti-human primary glucagon antibody (Sigma-Aldrich, St. Louis, MO), a polyclonal goat anti-human somatostatin primary antibody (Santa Cruz Biotechnology, Santa Cruz, CA) and DAPI (Invitrogen, Carlsbad, CA). The primary antibodies were detected using different combinations of Cy2, Cy5 and Texas Red-conjugated secondary antibodies (Jackson ImmunoResearch Laboratories, West Grove, PA). Microscopic images were taken with an Olympus IX81 DSU spinning disk confocal microscope (Melville, NY).

### Data analysis

Numbers of specimens and islets analyzed are as follows: human healthy adults ( $39 \pm 4.2$  yr,  $n = 3$ , 192 islets), rhesus monkey (1-yr,  $n = 2$ , 224 islets), pig (6-mo,  $n = 3$ , 285 islets), rabbit (6-mo,  $n = 3$ , 134 islets), mouse (wild-type, 6-mo,  $n = 3$ , 104 islets), song bird (40-d,  $n = 5$ , 80 islets), *db/db* mouse (15-wk,  $n = 3$ , 104 islets), *ob/ob* mouse (15-wk,  $n = 3$ , 158 islets), and pregnant mouse (3-mo,  $n = 3$ , 105 islets). Human pancreatic sections were sampled from the head region (nPOD). Sections shown for the various animals studied were randomly selected and are representative. Three dimensional scatter plots were generated using MATLAB (The MathWorks, Natick, MA). To quantify the difference in islet size distribution among species, we fitted the distributions with the lognormal function with two parameters,  $\mu$  and  $\sigma$ :

$$f(s) = \frac{1}{\sqrt{2\pi}\sigma} \frac{1}{s-10} \exp\left[-\frac{[\ln(s-10) - \ln\mu]^2}{2\sigma^2}\right]$$

Note that the islet size,  $s$ , is shifted with 10  $\mu\text{m}$  to reflect the biological distribution starts from a finite size, not zero. As a fitting routine, we used the nonlinear least-squares Marquardt-Levenberg algorithm provided by a GNUplot package.

### Statistical analysis

Statistical analyses were performed using nonpaired two-tailed student's t test. Differences were considered to be significant at  $p < 0.05$ .

### Acknowledgments

The authors thank Drs. Craig Wardrip and Marek Niekrasz, and Ms. Karin Peterson, Maggie Bruner and Jennifer McGrath, the Animal Resource Center, University of Chicago, and Mr. Patrick Moore for technical assistance. The

study is supported by US Public Health Service Grant DK-081527 and DK-20595 to the University of Chicago Diabetes Research and Training Center (Animals Models Core), and a gift from the Kovler Family Foundation.

## References

1. Brissova M, Fowler MJ, Nicholson WE, Chu A, Hirshberg B, Harlan DM, et al. Assessment of human pancreatic islet architecture and composition by laser scanning confocal microscopy. *J Histochem Cytochem* 2005;53:1087–97. [PubMed: 15923354]
2. Cabrera O, Berman DM, Kenyon NS, Ricordi C, Berggren PO, Caicedo A. The unique cytoarchitecture of human pancreatic islets has implications for islet cell function. *Proc Natl Acad Sci USA* 2006;103:2334–9. [PubMed: 16461897]
3. Orci L, Unger RH. Functional subdivision of islets of Langerhans and possible role of D Cells. *Lancet* 1975;2:1243–4. [PubMed: 53729]
4. Samols E, Bonner-Weir S, Weir GC. Intra-islet insulin-glucagon-somatostatin relationships. *Clin Endocrinol Metab* 1986;15:33–58. [PubMed: 2869846]
5. Yukawa M, Takeuchi T, Watanabe T, Kitamura S. Proportions of Various Endocrine Cells in the Pancreatic Islets of Wood Mice. *Anat Histol Embryol* 1999;28:13–6. [PubMed: 10208028]
6. Wieczorek G, Pospischil A, Perentes E. A comparative immunohistochemical study of pancreatic islets in laboratory animals (rats, dogs, minipigs, nonhuman primates). *Exp Toxicol Pathol* 1998;50:151–72. [PubMed: 9681646]
7. Sujatha SR, Pulimood A, Gunasekaran S. Comparative immunocytochemistry of isolated rat and monkey pancreatic islet cell types. *Indian J Med Res* 2004;119:38–44. [PubMed: 14997993]
8. Sánchez A, Cenani S, von Lawzewitsch I. Pancreatic islets in *Platyrrhini* monkeys: *Callithrix jacchus*, *Saimiri boliviensis*, *Aotus azarae* and *Cebus apella*. A cytological and immunocytochemical study. *Primates* 1991;32:93–103.
9. Pfister K, Rossi GL, Freudiger U, Bigler B. Morphological studies in dogs with chronic pancreatic insufficiency. *Virchows Arch A Pathol Anat Histol* 1980;386:91–105. [PubMed: 6996311]
10. Hawkins KL, Summers BA, Kuhajda FP, Smith CA. Immunocytochemistry of normal pancreatic islets and spontaneous islet cell tumors in dogs. *Vet Pathol* 1987;24:170–9. [PubMed: 2883753]
11. Kuroda Y, Suzuki Y, Kawamura T, Fujiwara H, Fujino Y, Yamamoto K, et al. The long-term function and histology of segmental pancreatic autografts with pancreatic exocrine diversion to the esophagus in dogs. *Jpn J Surg* 1990;20:685–9. [PubMed: 2084292]
12. Bonner-Weir S. Regulation of pancreatic beta-cell mass in vivo. *Recent Prog Horm Res* 1994;49:91–104. [PubMed: 8146438]
13. Montanya E, Nacher V, Biarnés M, Soler J. Linear correlation between beta-cell mass and body weight throughout the lifespan in Lewis rats: role of beta-cell hyperplasia and hypertrophy. *Diabetes* 2000;49:1341–6. [PubMed: 10923635]
14. Takei S, Teruya M, Grunewald A, Garcia R, Chan EK, Charles MA. Isolation and function of human and pig islets. *Pancreas* 1994;9:150–6. [PubMed: 8190716]
15. Kenmochi T, Miyamoto M, Une S, Nakagawa Y, Moldovan S, Navarro RA, et al. Improved quality and yield of islets isolated from human pancreata using a two-step digestion method. *Pancreas* 2000;20:184–90. [PubMed: 10707935]
16. Bonner-Weir S. Morphological evidence for pancreatic polarity of beta-cell within islets of Langerhans. *Diabetes* 1988;37:616–21. [PubMed: 3282948]
17. Stagner JI, Samols E. Retrograde perfusion as a model for testing the relative effects of glucose versus insulin on the A cell. *J Clin Invest* 1986;77:1034–7. [PubMed: 3512599]
18. Stagner JI, Samols E, Marks V. The anterograde and retrograde infusion of glucagon antibodies suggests that A cells are vascularly perfused before D cells within the rat islet. *Diabetologia* 1989;32:203–6. [PubMed: 2568960]
19. Murakami T, Fujita T, Miyake T, Ohtsuka A, Taguchi T, Kikuta A. The insulo-acinar portal and insulovenous drainage systems in the pancreas of the mouse, dog, monkey and certain other animals: a scanning electron microscopic study of corrosion casts. *Arch Histol Cytol* 1993;56:127–47. [PubMed: 8373657]

20. Miyake T, Murakami T, Ohtsuka A. Incomplete vascular casting for a scanning electron microscope study of the microcirculatory patterns in the rat pancreas. *Arch Histol Cytol* 1992;55:397–406. [PubMed: 1482604]
21. Ohtani O. Review of scanning electron and light microscopic methods in microcirculation research and their application in pancreatic studies. *Scan Electron Microsc* 1984;2:653–61. [PubMed: 6385219]
22. Brunnicardi FC, Stagner J, Bonner-Weir S, Wayland H, Kleinman R, et al. Microcirculation of the islets of Langerhans. Long Beach Veterans Administration Regional Medical Education Center Symposium. *Diabetes* 1996;45:385–92. [PubMed: 8603757]
23. Ballian N, Brunnicardi FC. Islet vasculature as a regulator of endocrine pancreas function. *World J Surg* 2007;31:705–14. [PubMed: 17347899]
24. Samols E, Stagner JI, Ewart RB, Marks V. The order of islet microvascular cellular perfusion is B----A----D in the perfused rat pancreas. *J Clin Invest* 1988;82:350–3. [PubMed: 2455737]
25. Aharinejad S, MacDonald IC, Schmidt EE, Böck P, Hagen D, Groom AC. Scanning and transmission electron microscopy and high resolution intravital video-microscopy of capillaries in the mouse exocrine pancreas, with special emphasis on endothelial cells. *Anat Rec* 1993;237:163–77. [PubMed: 8238968]
26. Liu YM, Guth PH, Kaneko K, Livingston EH, Brunnicardi FC. Dynamic in vivo observation of rat islet microcirculation. *Pancreas* 1993;8:15–21. [PubMed: 8419903]
27. Nyman LR, Wells KS, Head WS, McCaughey M, Ford E, Brissova M, et al. Real-time, multidimensional in vivo imaging used to investigate blood flow in mouse pancreatic islets. *J Clin Invest* 2008;118:3790–7. [PubMed: 18846254]
28. Edvell A, Lindstrom P. Development of insulin secretory function in young obese hyperglycemic mice (Umea ob/ob). *Metabolism* 1995;44:906–13. [PubMed: 7616850]
29. Pick A, Clark J, Kubstrup C, Levisetti M, Pugh W, Bonner-Weir S, et al. Role of apoptosis in failure of beta-cell mass compensation for insulin resistance and beta-cell defects in the male Zucker diabetic fatty rat. *Diabetes* 1998;47:358–64. [PubMed: 9519740]
30. Parsons NA, Brejle TC, Sorenson RL. Adaptation of islets of Langerhans to pregnancy: increased islet cell proliferation and insulin secretion correlates with the onset of placental lactogen secretion. *Endocrinology* 1992;130:1459–66. [PubMed: 1537300]
31. Karnik SK, Chen H, McLean GW, Heit JJ, Gu X, Zhang AY, et al. Menin controls growth of pancreatic beta-cells in pregnant mice and promotes gestational diabetes mellitus. *Science* 2007;318:806–9. [PubMed: 17975067]
32. Bock T, Pakkenberg B, Buschard K. Increased islet volume but unchanged islet number in ob/ob mice. *Diabetes* 2003;52:1716–22. [PubMed: 12829638]

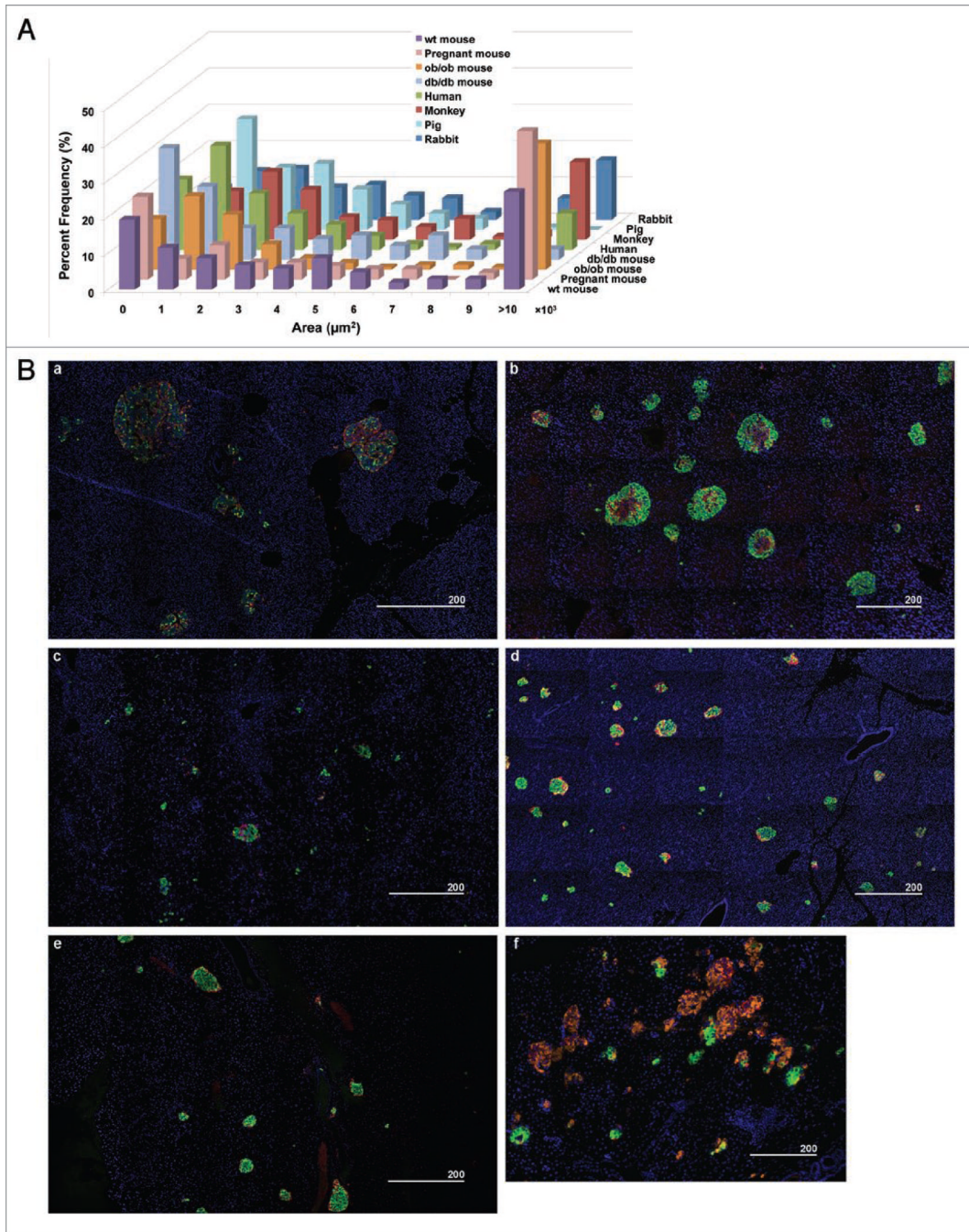


**Figure 1.**

Immunohistochemical analysis of pancreatic islets from various species. (A) Islet size distribution across several species including *ob/ob*, *db/db* and pregnant mice. Note the similar distribution pattern within the closely overlapping range in size among species. (B) Immunofluorescent staining of insulin (green), glucagon (red), somatostatin (orange) and nuclei (blue) showing an overview of islet distribution in each species. (a) Human, (b) Rhesus monkey, (c) Pig, (d) Rabbit, (e) Mouse, (f) Song bird. Scale in  $\mu\text{m}$ .



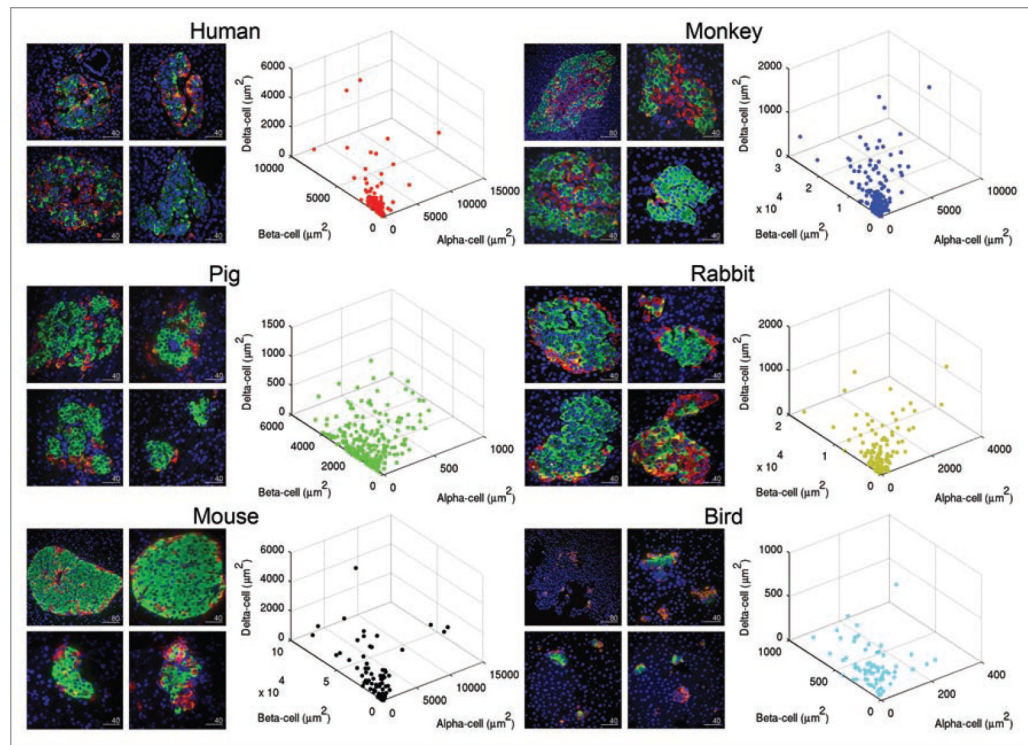


**Figure 2.**

Plasticity and variability of islet in various species. Representative islets of each species are shown on the left, and distribution of islets according to endocrine cell composition is plotted in 3D on the right. Each dot depicts a single islet. Note the diversity of islet size, shape and cell composition among species as well as within the same species, demonstrating the plasticity and variability of islets. For birds, islets with beta-cells were selectively shown. Scale in  $\mu\text{m}$ .

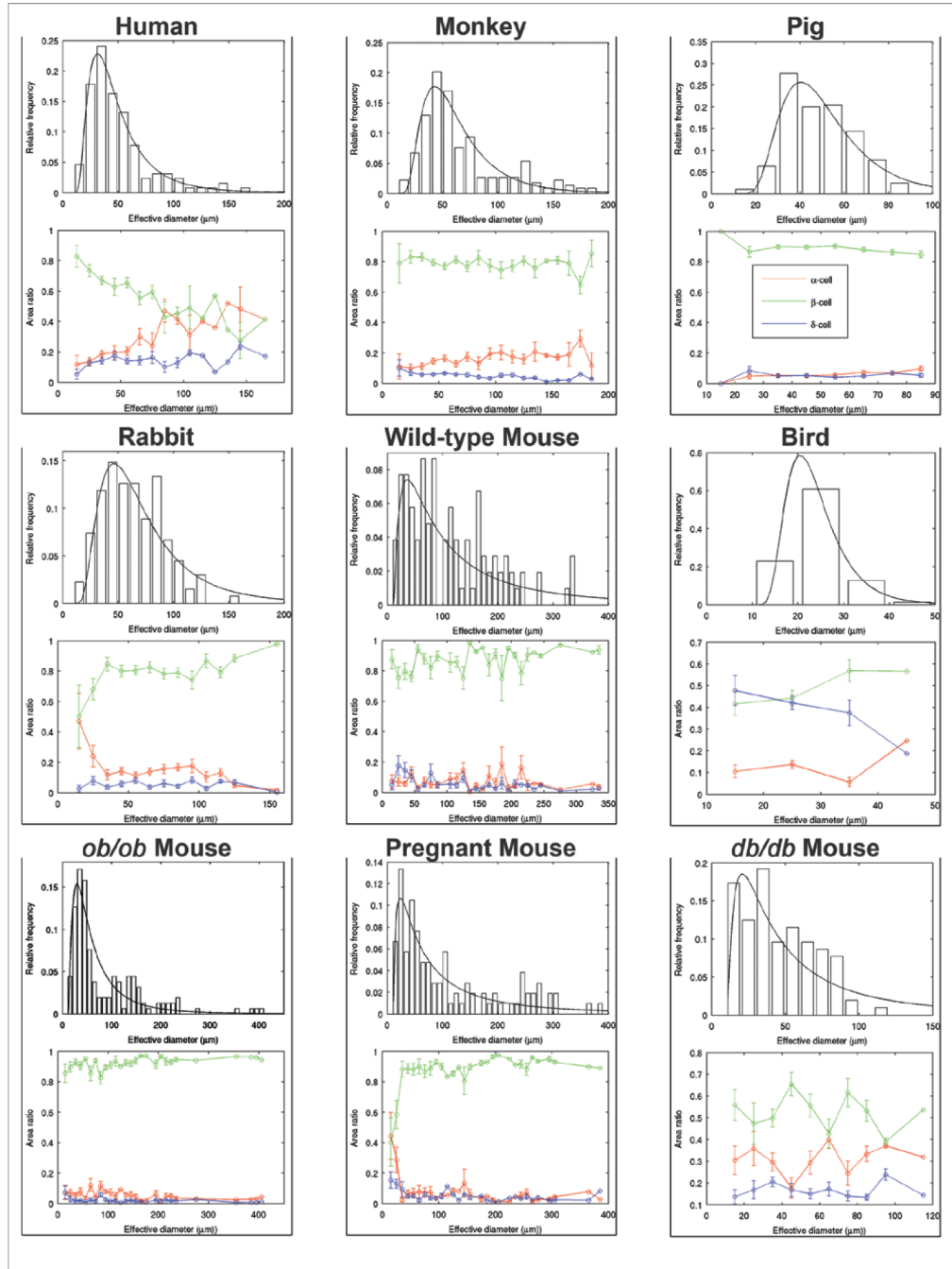


**Figure 3.** Mathematical analysis on islet size distribution and cellular composition among species. Top: lognormal probability density functions are fitted to histograms of islet effective diameters (i.e., a parameter that depicts the same area of a theoretical perfect circle) for each species. Bottom: cellular composition ratios ( $\beta$ -cells in green,  $\alpha$ -cells in red and  $\delta$ -cells in blue) for each islet effective diameter bin.

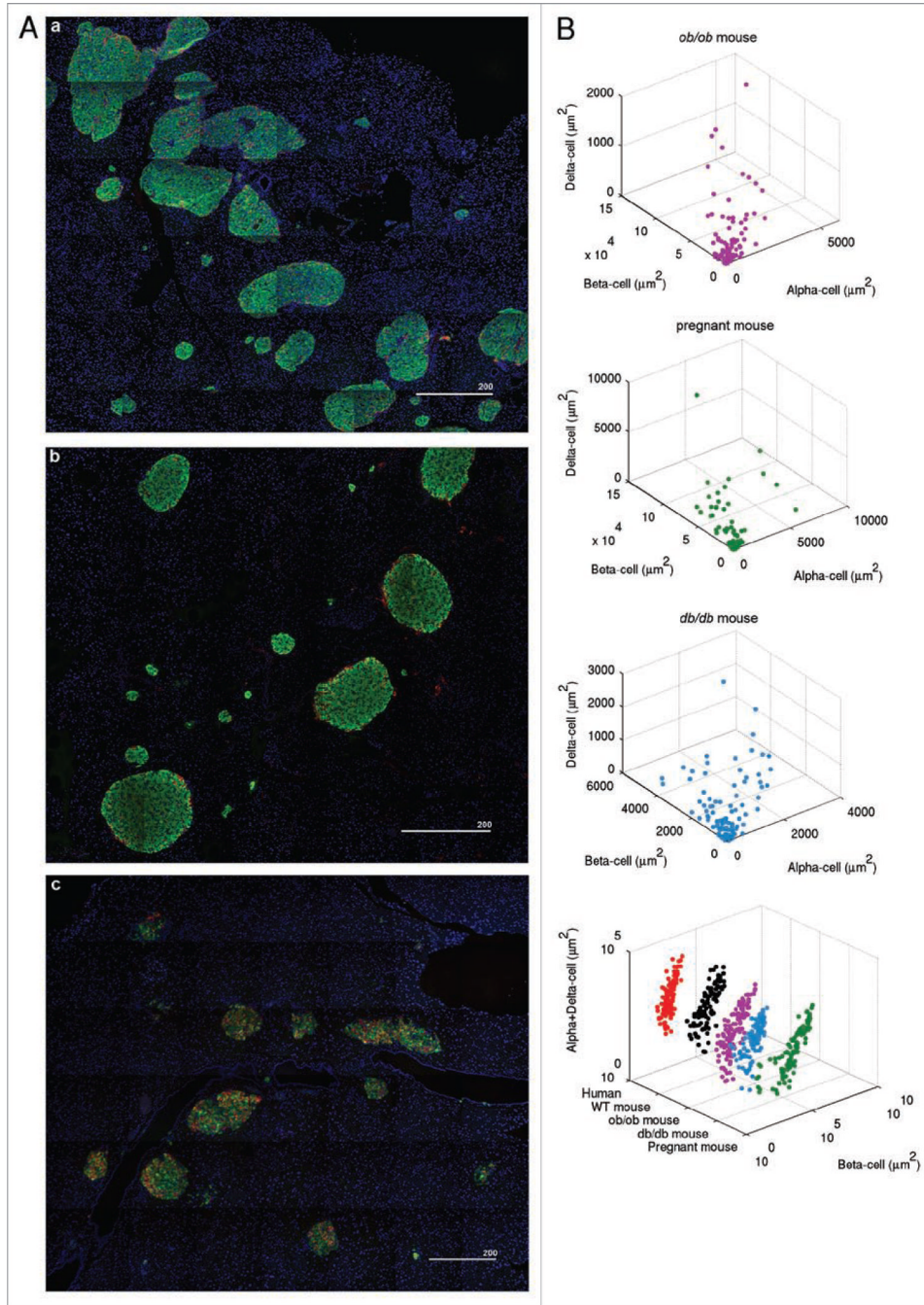


**Figure 4.** Changes in islet architecture and composition under pathophysiological conditions such as obesity, pregnancy and diabetes. (A) Overviews of islet distribution in *ob/ob* (a), pregnant (b) and *db/db* (c) mice. Scale in  $\mu\text{m}$ . (B) Corresponding 3D scatter plots to images in (A) are shown. Distribution of endocrine cell composition is compared between human and mice under normal and pathophysiological conditions (lower left). Note the similarities in islet size distribution and islet composition between humans and mice.

**Table 1**Islet size and  $\beta$ -cell ratio for different species

Species	Islet size ( $\mu\text{m}$ )	$\beta$ -cell ratio	$\mu$	$\sigma$
Human	$50 \pm 29$	$0.64 \pm 0.21$	$33 \pm 1$	$0.66 \pm 0.03$
Monkey	$67 \pm 38^*$	$0.79 \pm 0.14^*$	$46 \pm 2$	$0.58 \pm 0.04$
Pig	$49 \pm 15^a$	$0.89 \pm 0.11^*$	$38 \pm 2$	$0.46 \pm 0.04$
Rabbit	$64 \pm 28^*$	$0.79 \pm 0.17^*$	$53 \pm 3$	$0.62 \pm 0.05$
Bird	$24 \pm 6^*$	$0.46 \pm 0.24^*$	$13 \pm 1$	$0.44 \pm 0.04$
Wild-type mouse	$116 \pm 80^*$	$0.85 \pm 0.14^*$	$90 \pm 12$	$1.11 \pm 0.11$
<i>ob/ob</i> mouse	$86 \pm 76^*$	$0.92 \pm 0.11^*$	$43 \pm 3$	$0.90 \pm 0.05$
<i>db/db</i> mouse	$47 \pm 24^b$	$0.53 \pm 0.24^c$	$36 \pm 6$	$1.10 \pm 0.14$
Pregnant mouse	$112 \pm 94^*$	$0.84 \pm 0.22^*$	$66 \pm 7$	$1.25 \pm 0.08$

Islet size is described as an effective diameter of a circle, which depicts the same area as a measured islet area.  $\beta$ -cell ratio is the area ratio of  $\beta$ -cells in an islet. Both data sets are expressed as the mean value with its standard deviation. Islet size distribution is fitted with the lognormal function with two parameters describing the peak position,  $\mu$ , and the x-axis scale,  $\sigma$ . Error of the parameter values is an asymptotic standard error calculated from the fitting routine of GNUplot.

\*  $p < 0.0001$  compared with human.

<sup>a</sup>  $p = 0.65$

<sup>b</sup>  $p = 0.42$

<sup>c</sup>  $p = 0.0004$